

BNL Collider-Accelerator Department
Accelerator Physics Seminar
August 14, 2008

**Energy-Doubled Bragg Scattering, CESR-X/FEL,
and Depth-Selective X-Ray Diffraction**

Richard Talman

CORNELL LABORATORY OF ELEMENTARY-PARTICLE PHYSICS

Contents

- 1. Introduction
- 2. Energy-Doubled Bragg Scattering
 - 2.1. The Laue Equations
 - 2.2. Hyper-Rayleigh Molecular Cross Section
 - 2.3. Intensity Enhancement by X-Ray Lenses
- 3. Experimental Details
 - 3.1. CESR-X
 - 3.2. Plan of Apparatus
 - 3.3. Bunch Shortening
 - 3.4. Splitting and Corrugating the Electron Beam
 - 3.5. Pulsed Wavefront Straightening
 - 3.6. Undulator
- 4. Rate Calculations
 - 4.1. Bunch Charge and Current Achievable in CESR-X
 - 4.2. Can CESR-X Operate as an FEL?

Abstract

An intense photon beam incident on a molecule can produce hyper-Rayleigh scattering in which two incident photons effectively merge, and a single energy-doubled photon is produced. Though routinely visible with visible light, the intensity and coherency of x-ray beams has always been too low (by more than 10 orders of magnitude) for energy doubling to be detectible with Ångstrom x-rays. A scheme is described for overcoming this *10 orders of magnitude challenge* to observe the effect. The same gigantic factor that enhances Bragg scattering from crystals will make the effect observable in CESR-X/FEL (an upgraded version of the Cornell storage ring) or at similarly-configured free electron lasers. More challenging than the *production* of energy-doubling is its *detection* in the sea of normal x-ray scatters. Taking advantage of the doubled energy, sufficient background rejection is also enabled by Bragg energy and angle selectivity.

A plan is then described for *increasing* the signal instead of *decreasing* the background, by producing very intense x-ray pulses. From an equilibrium state with huge bunch charge circulating in CESR-X (but with charge density diluted to suppress the Touschek effect, premature lasing, and wall heating) the bunch length is reduced to small values, first slowly over several milliseconds, then suddenly over a single turn. Then, with the help of a high power visible laser pulse the beam is split into the two coherent beams needed for the (futuristic) interferometric applications that can exploit the energy doubling process.

Alternative modes of operation are possible with the same equipment. For example, femtosecond-scale x-ray pulses can be produced, though at greatly reduced intensity. Or, with sub-critical charge per bunch, but factor-of-ten bunch compression, sub-picosecond, but otherwise conventional, full-intensity, x-ray pulses will be produced—ideal for all but the most extreme time-resolution pump-probe experiments. Finally, single beam FEL operation, with its gigantic peak brilliance should be possible.

Many of these features can be achieved non-destructively, with the circulating beam given several milliseconds to recover from the torture to which it has been subjected, before the torture is re-applied. This will be the preferred mode of operation, with ~ 1 kHz repetition rate. But, to achieve truly huge intensities, the beam will be irreparably damaged and will need to be re-injected. In this mode the anticipated huge peak brilliance can be expected to compensate for the thousand-fold reduction in repetition rate, though at the (usual) cost of irreproducible FEL operation.

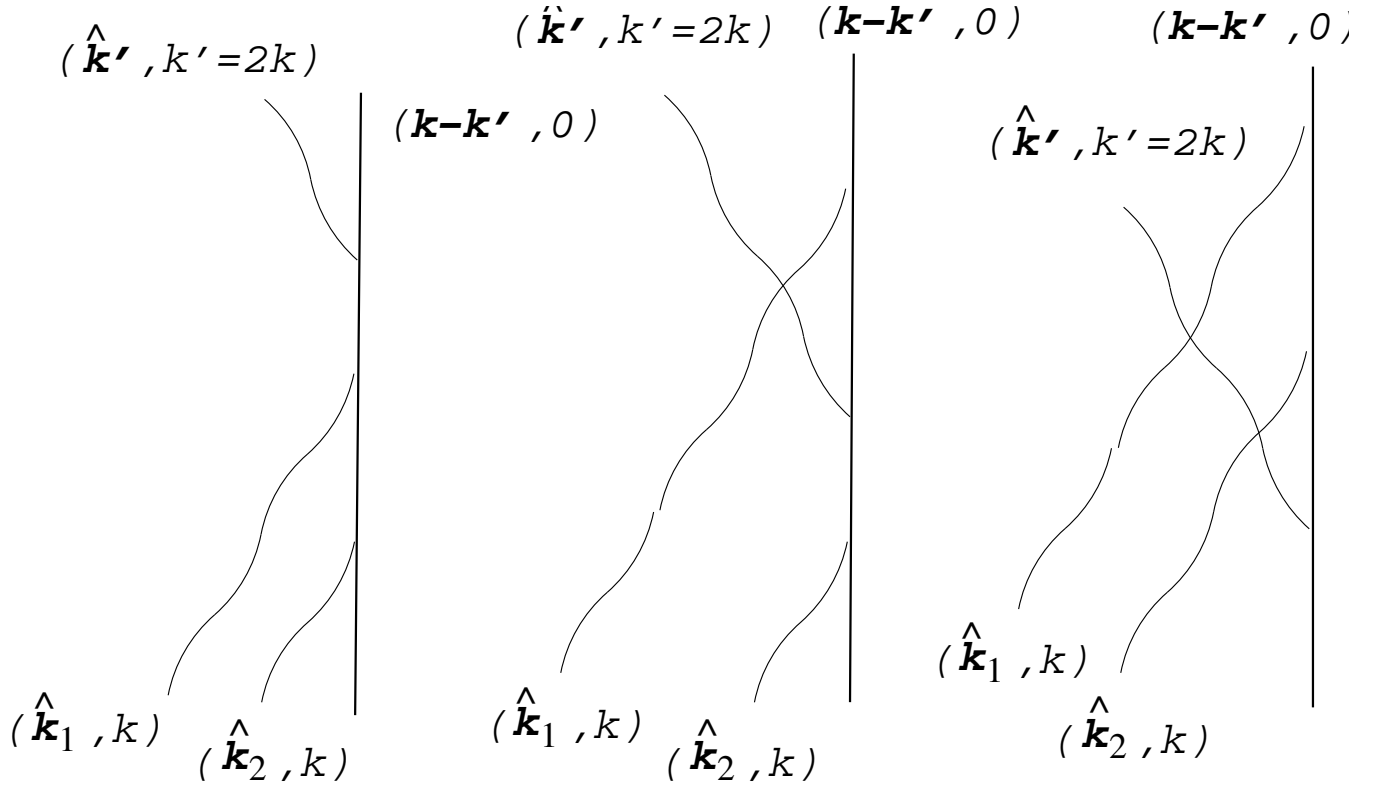


FIGURE 1. Feynmann diagrams for hyper-Rayleigh scattering. The same diagrams apply just as well to hyper-Compton scattering, in which case the heavy line represents a free electron. In the simplest experimental configuration $\hat{\mathbf{k}}_1$ and $\hat{\mathbf{k}}_2$ are identical, but they need not be.

Energy-Doubled Bragg Scattering

For incident light of wavelength $\lambda = 2\pi/k$, the radiated power per unit solid angle for scattering from a molecule is given by

$$(1) \quad \frac{dP'}{d\Omega'} = \frac{\bar{I}_0^2 g^{(2)} k^4}{2\pi^2 \epsilon_0^3 c} |\vec{e}'_i e_j e_k < N \beta_{ijk} >|^2.$$

where \bar{I}_0^2 is the average squared-incident-power per unit area per unit frequency interval. At “critical laser intensity” I_c^L normal- and hyper- production rates are roughly equal:

$$(2) \quad I_c^L = \frac{\alpha \hbar \omega_L^2}{8\pi r_0^2}.$$

where A_0^L is the amplitude of the incident wave.

$$I_c^L[\hbar\omega_L=0.1 \text{ eV}] = 10^{16} \text{ W/cm}^2$$

$$I_c^L[\hbar\omega_L=1 \text{ eV}] = 10^{18} \text{ W/cm}^2$$

$$I_c^L[\hbar\omega_L=10 \text{ keV}] = 10^{26} \text{ W/cm}^2$$

Hyper-Rayleigh scattering from molecules depends on deviation from Hooke's law of the "springs" holding electrons in place.

Bragg scattering is quite the opposite. The electrons can be treated as free. Even so, their recoil is taken up by the crystal. Same Feynmann diagrams though.

Anharmonic response depends on the magnetic force being substantial, which requires relativistic electron speed (further discriminating against x-rays because of their high frequency.)

The condition for scattering from all atoms in a crystal to be coherent (Bragg) is the same as the condition for the scattering from each atom to be elastic.

Make up 10 orders of magnitude in rate by using crystal diffraction both to increase the foreground (hyper-Bragg) and to reduce the background (ordinary Thomson).

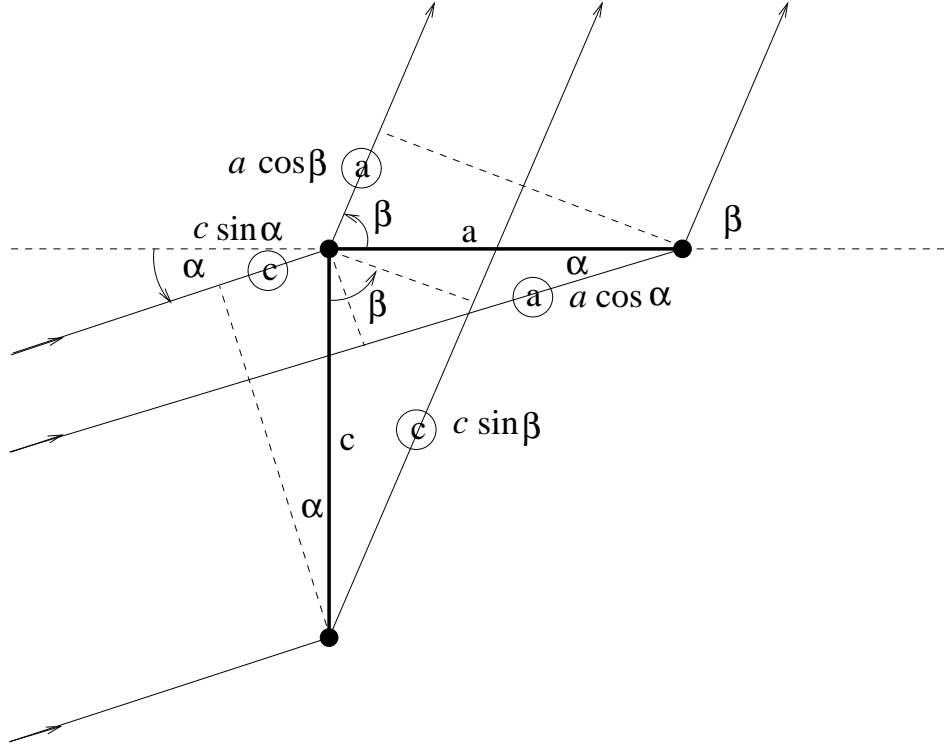


FIGURE 2. Derivation of the Laue equations for hyper-Bragg scattering.

For scattering from the a -separated atoms to be constructive, the length of the pre-scatter leg labeled with a circled a , when measured in units of λ , must differ by an integer n_a from the length of the post-scattered leg labeled with a circled a , but measured in units of $\lambda/2$. Ditto for c -separated atoms.

$$(3) \quad \frac{a \cos \alpha}{\lambda} - \frac{a \cos \beta}{\lambda/2} = n_a, \quad \text{or} \quad \cos \alpha - 2 \cos \beta = n_a \frac{\lambda}{a}.$$

$$(4) \quad \frac{c \sin \alpha}{\lambda} - \frac{c \sin \beta}{\lambda/2} = n_c, \quad \text{or} \quad \sin \alpha - 2 \sin \beta = n_c \frac{\lambda}{c}.$$

Angle of “reflection” is *not* equal to angle of incidence. Ewald sphere construction is *not* applicable.

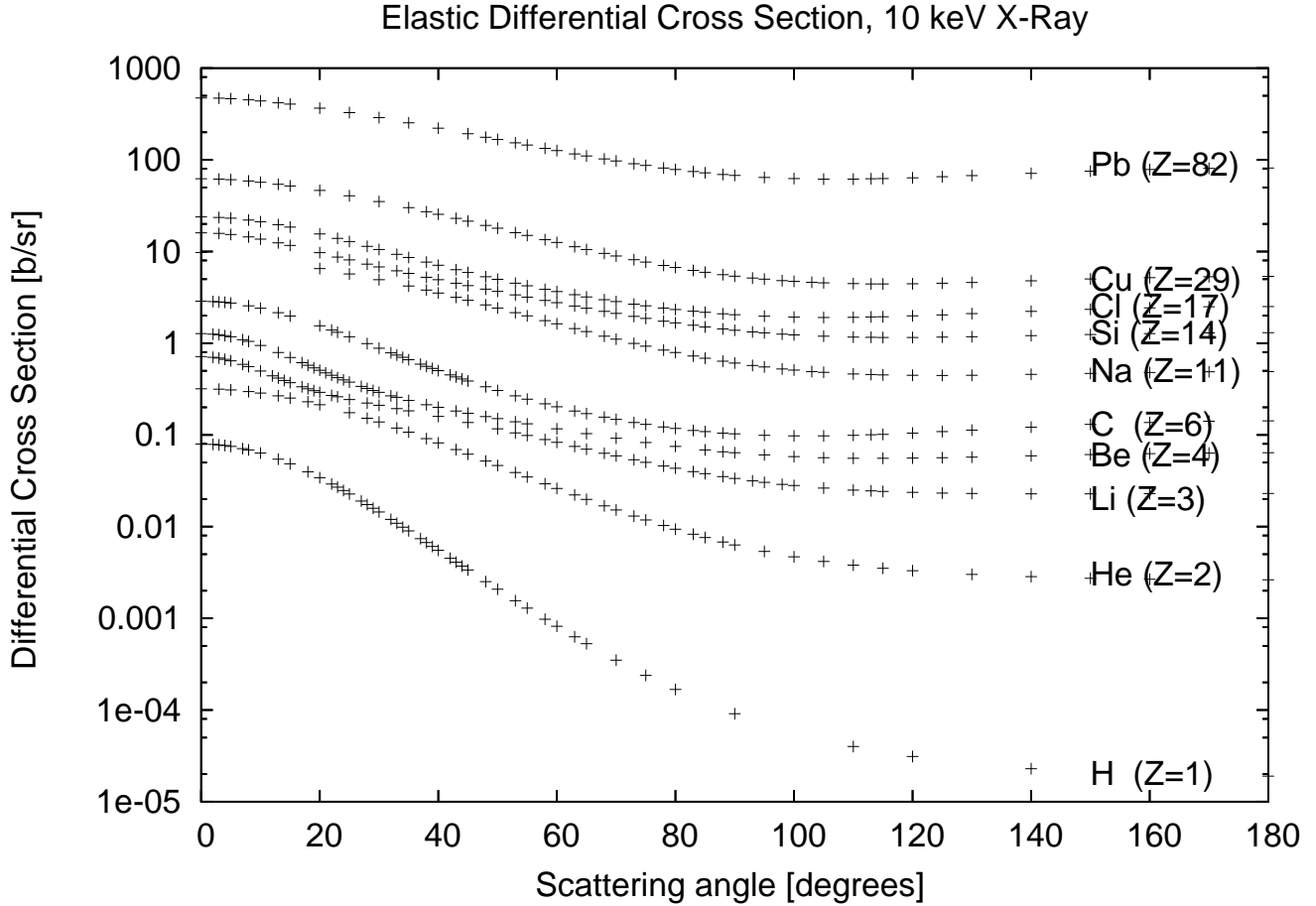


FIGURE 3. The hydrogen atoms (important in all organic materials) compete badly in x-ray diffraction at all angles. (Meanwhile neutron diffraction shines.) ASIDE: Hydrogen will compete far better when the transverse recoil momentum is canceled in the two beam hyper-Bragg process—the form factor will be close to 1.

But, for hyper-Bragg to be practical as a tool, we have to increase the foreground (by increasing I^L).

Pump-Probe Rate Considerations

We have a “pump-probe” situation. with the same beam acting as both pump and probe, and with the delay between pump and probe being 0 fs. Assuming constant bunch dimensions, the instantaneous data rate is proportional to the product of two peak currents \mathcal{I}_1 and \mathcal{I}_2 , assumed to scale proportionally. At *fixed average power*, the peak currents and bunch passage rate ν_{rep} are related by $\mathcal{I} \sim 1/\nu_{rep}$.

Counts C_n needed (to observe some phenomenon) and time needed T_n (to accumulate that many counts) are related by

$$(5) \quad T_n \sim \frac{C_n}{\mathcal{I}_1 \mathcal{I}_2 \nu_{rep}}.$$

Biological damage D scales as

$$(6) \quad D \sim \mathcal{I}_1 \nu_{rep} T_n.$$

Increasing charge per bunch by factor m , ν_{rep} decreases proportionally, giving $\mathcal{I}_{1,2} \rightarrow m\mathcal{I}_{1,2}$ and, as a result

$$(7) \quad T_n \rightarrow \frac{T_n}{m}, \quad \text{yielding} \quad D \rightarrow \frac{D}{m}.$$

WE NEED TO MAXIMIZE BEAM CHARGE PER BUNCH (by reducing ν_{rep} and increasing charge per bunch to the extent possible.)

Big Numbers and Coherent Radiation

Most of the development revolves around a few *big numbers*. The relativistic factor for the CESR electrons is $\gamma_e = 10^4$. This big number enters comparisons between quantities measured in the laboratory frame and in the electron rest frame. The ratio of visible photon wavelengths to x-ray wavelengths is 10^4 , which (not coincidentally) is the same as the ratio of a micrometer (μm) to an Ångström. Of course the number of electrons in a bunch $N_e \approx 10^{11}$ is a *huge* number. Furthermore, with “microbunching” the N_e electrons will be segregated into an also-large number $\widetilde{m}_e \approx 10^5$ of sub-bunches. With some processes (incoherent) being proportional to \widetilde{N}_e and others (coherent) proportional to $\widetilde{M}_e^2 = (\widetilde{N}_e/\widetilde{m}_e)^2$, it should not be surprising that the bigness of these numbers is important.

The number of poles of an undulator $2N_w \approx 10^3$ is also a significantly large number. Associated with γ being big is the fact that a typical angle for synchrotron radiation is $1/\gamma = 10^{-4}$. When discussing the (coherent) photons of importance in this paper, their typical angle is reduced from $1/\gamma$ by another substantial factor $1/\sqrt{2N_w} \approx 1/30$.

CESR-X: In-Tunnel Conversion of CESR into Bright X-Ray Source

Ivan Bazarov, Yulin Li, Richard Talman,
Cornell Laboratory of Elementary-Particle Physics
Ken Finkelstein, Cornell High Energy Synchrotron Source
Lois Pollack, Cornell Department of Applied and Engineering Physics
Ken Soong, Cornell Physics Department

March 29, 2008

Contents

1	Introduction	4
1.1	Motivation, Schedule, and Parameters	4
1.2	Performance as X-Ray Source	7
1.2.1	Brilliance	7
1.2.2	Coherence	9
1.2.3	Timing	11
2	Lattice Properties	12
2.1	Design Strategy	12
2.2	SRF Cryomodules	13
2.3	Beam Transfer From the Synchrotron to CESR-X	13
2.4	Nudging the CESR-X Lattice onto the CESR Footprint	14
3	Longitudinal Parameters	23
3.1	RF and the Damping Wiggler Option	24
4	Required New and Rebuilt Hardware	24
4.1	Bending Magnets	24
4.2	Quadrupoles	28
4.3	Vacuum System	31
5	Notes on Costs	36
5.1	General Comments	36
5.2	Magnet Counts	37

6	X-Ray Beamlines	39
6.1	CESR-X-Specific Undulator Design	39
6.2	Dual Canted Undulator X-Ray Lines	39
6.3	Beamline Parameters	39
7	Science Opportunities With CESR-X	43
7.1	Introduction	43
7.2	Inelastic X-ray Scattering	43
7.3	High Pressure Science	44
7.4	Resonant Scattering in Pump-Probe Mode	44
7.5	Pair-Distribution Function (PDF)	45
7.6	Measurement of Transient Intermediates Along the Folding Path- ways of Proteins, RNA or DNA	46
7.7	Scientific Impact	47
8	Near Term Tasks	47

TABLE 1. CESR-X parameters.

Parameter	Symbol	Unit	Wiggler Option
beam energy	\mathcal{E}_e	GeV	5.0
beam current	I_e	A	0.2
stored charge	Q_e	C	5×10^{-7}
magnetic field	B	T	0.384
bend radius	ρ	m	43.44
cell bend length	L_b	m	6.498
bend angle per cell		r	$2\pi/42$
circumference	C	m	763.74
horizontal tune	Q_x		38.90
vertical tune	Q_y		20.68
longitudinal tune	Q_z		0.009
r.m.s. energy spread	σ_δ		0.00065
r.m.s. bunch length	σ_{ct}	mm	2.9
1/transition-gamma-sq.	$1/\gamma_{tr.}^2$		3.84e-4
horizontal emittance	ϵ_x	nm	1.6
vertical emittance	ϵ_y	pm	16
energy loss per turn	U_0	MeV	2.506
radiated power		MW	0.50
vert. damping lifetime	$1/\alpha_y$	turns	1964
max. dispersion	$D_{\max.}$	m	0.2
min. dispersion	$D_{\min.}$	m	0
max. brilliance @10. keV	$\mathcal{B}_{\max.}$	$\frac{10^{20} \text{photons}}{\text{s mm}^2 \text{ mrad}^2 0.1\% \text{B.W.}}$	≈ 80

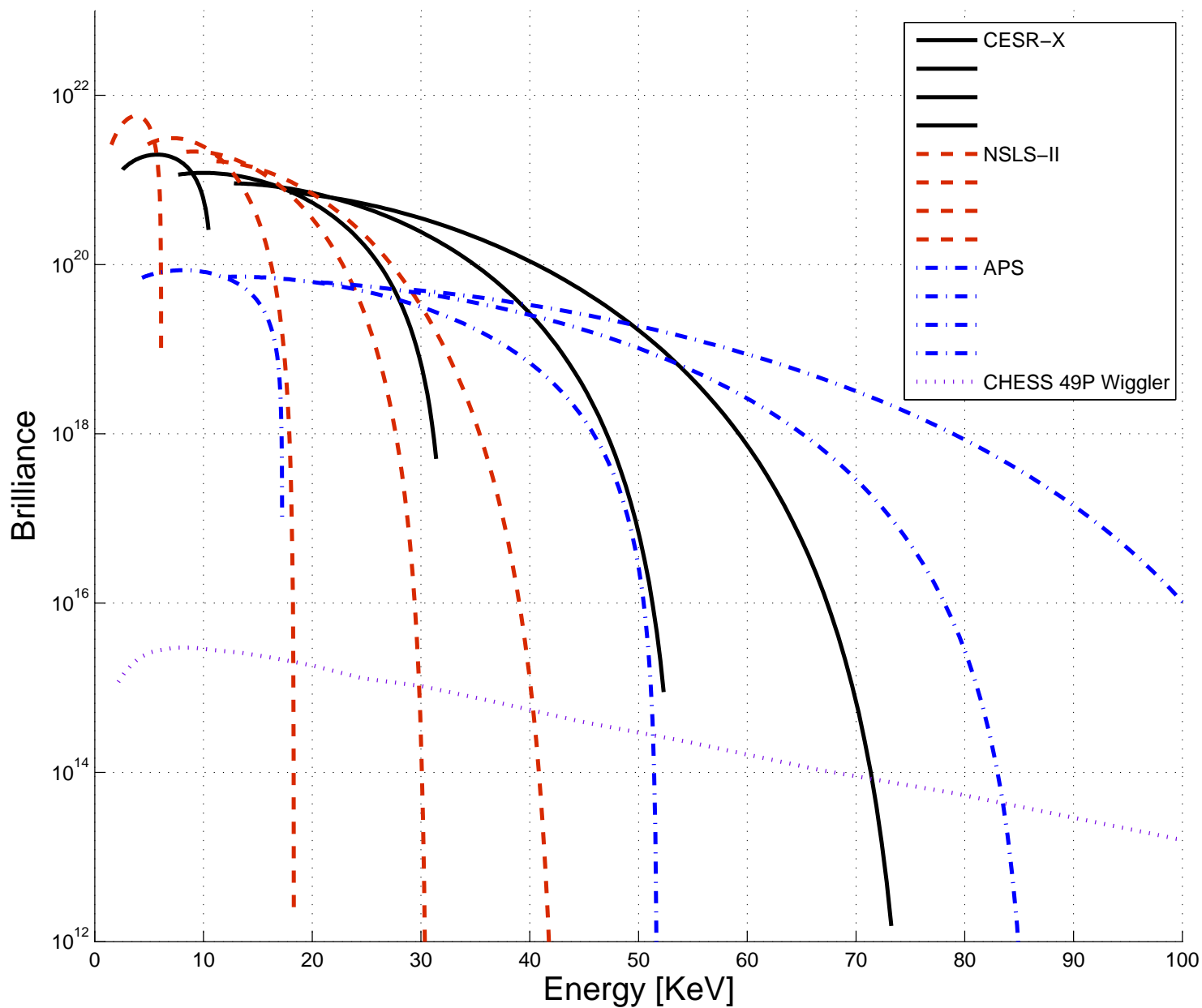
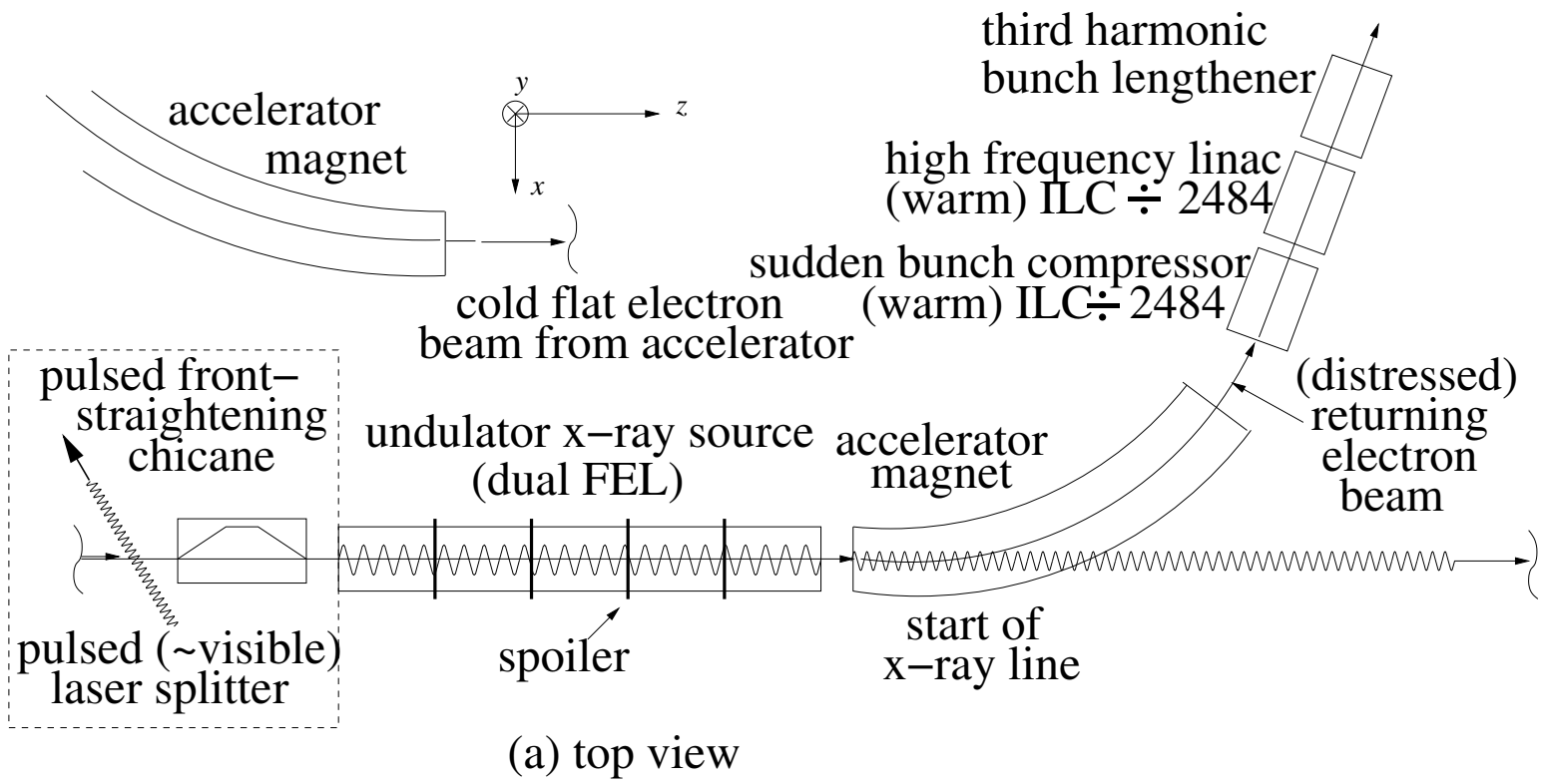
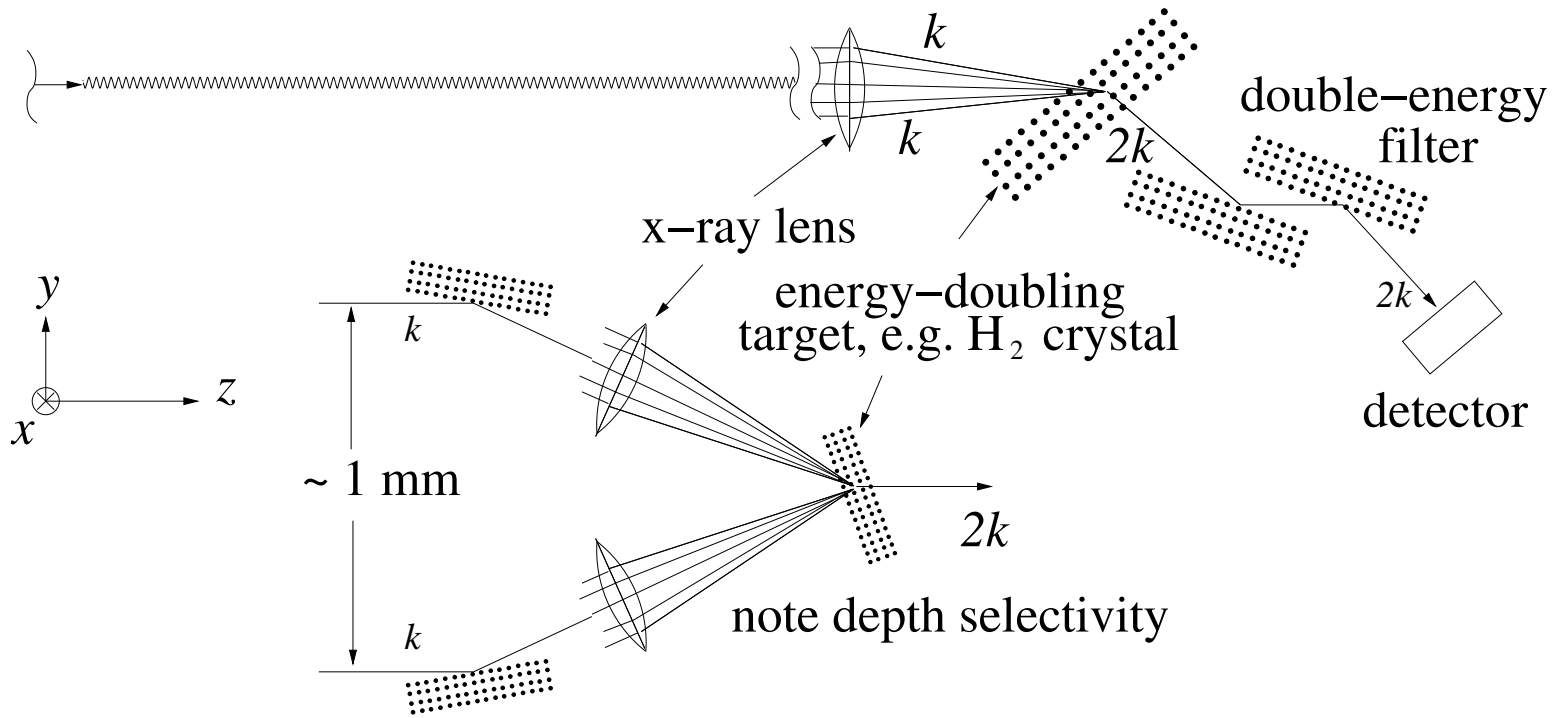


FIGURE 4. Brilliance curves for NSLS-II, CERN-X, and APS as calculated by SPECTRA8. Installing CERN-C wigglers will triple all CERN-X brilliances.





(b) side view, interferometric configuration

Superpowers enabled by hyper-Bragg process

Ability to “see” the hydrogen atoms in organic crystals—by canceling transverse momentum.

Ability to see internal structures, unobscured by preceeding dense material.

Ability to diffract selectively from inner layers.

But it works only at high beam intensity.

Variable	system	quantity	nominal value
$(w_e, h_e, \widetilde{l_e})$ (ϵ_x, ϵ_y) $(\langle \beta_x \rangle, \langle \beta_y \rangle)$ $(\widetilde{N_e}, \widetilde{M_e}, \widetilde{m_e})$	electrons	r.m.s. dimensions geometric emittances β functions at undulator particle/bunch numbers	$(30, 3, 3000) \mu\text{m}$ $(1, 0.01) \text{ nm}$ $(3.6, 3.6) \text{ m}$ $(1e11^*, 0.83e7, 2 \times 6000)$
(w_L, h_L, l_L) $(\eta_{L,w}, \eta_{L,h}, \eta_{L,l})$ λ_L θ_L U_L $(E_{\text{max.}}, B_{\text{max.}})$ $\Delta\psi_{\text{max.}}$	laser	r.m.s. dimensions wavelength angle (relative to normal) energy/pulse maximum fields max. electric deflection	$(0.13, 3, 1e4) \mu\text{m}$ $(1, 5, 2)$ $0.8 \mu\text{m}$ 80 degrees 1 J $(1e12 \text{ V/m}, 0.3e4 \text{ T})$ $50 \mu\text{r}$
$(\nu_{\text{lin.}}, \lambda_{\text{lin.}}, \mathcal{E}_{\text{max.}})$ $(2a_{\text{lin.}}, L_{\text{lin.}})$ $(t_{\text{fill}}, \nu_{\text{fill}})$	bunch-compressing linac	parameters (bore diam., section len.) (filling time, rep. rate)	$(11.42 \text{ GHz}, 2.63 \text{ cm}, 71 \text{ MeV})$ $(9 \text{ mm}, 1.8 \text{ m})$ $(100 \text{ ns}, 120 \text{ Hz})$
$(L_{\text{chic.}}, \Delta\theta_F)$	front-squaring chicane	(length, correction angle)	$(4 \text{ m}, 5 \text{ degrees})$
(W_w, H_w, L_w) (N_w, λ_w) $(B_w, R_w, \widetilde{K_w})$	undulator/ wiggler	dimensions parameters	$(\text{n.a.}, 5 \text{ mm}, 8 \text{ m})$ $(400, 2 \text{ cm})$ $(0.54 \text{ T}, 31 \text{ m}, 1)$
$\widetilde{L_{\text{b.l.}}}$	beam line	length	$\overset{e.g}{=} 50 \text{ m}$
$(w_\gamma, h_\gamma, l_\gamma)$ $(\lambda_\gamma, \mathcal{E}_\gamma)$ $(\Delta\theta_\gamma, \Delta\psi_\gamma)$	incoherent x-ray beam	dimensions (wavelength, energy) half-angles	$(30, 3, 150) \mu\text{m}$ $(1 \text{ \AA}, 12 \text{ keV})$ $(3.5, 3.5) \mu\text{r}$
$(\lambda_\gamma, \mathcal{E}_\gamma)$ $(w_{\text{coh}}, h_{\text{coh}}, l_{\text{coh}})$	FEL x-ray beam	(wavelength, energy) coherence dimensions	$(1 \text{ \AA}, 12 \text{ keV})$
(M_x, M_y) (w_T, h_T, l_T)	x-ray lens and target	1/magnification factors focussed coherence dim's	$(2000, 200)$ $() \mu\text{m}$

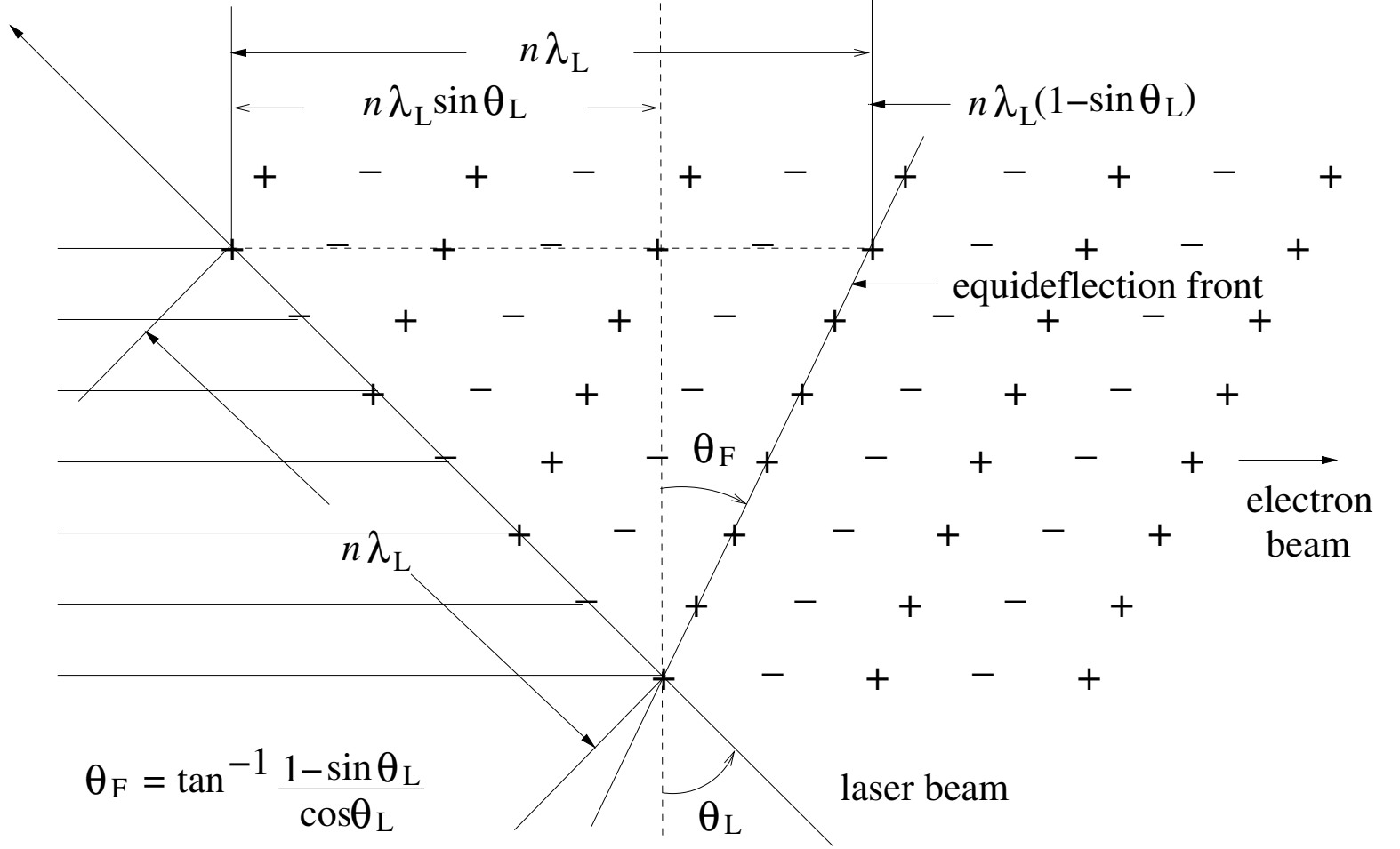


FIGURE 5. As the electron beam passes through the (temporarily) continuous (approximately visible light) laser beam they are deflected, some up, some down, as indicated by “+/-” signs. With laser beam incident at angle θ_L , the equideflection front is oriented at angle θ_F . This front still needs to be straightened by the pulsed chicane. Increasing θ_L reduces θ_F which relaxes the demand on the chicane.

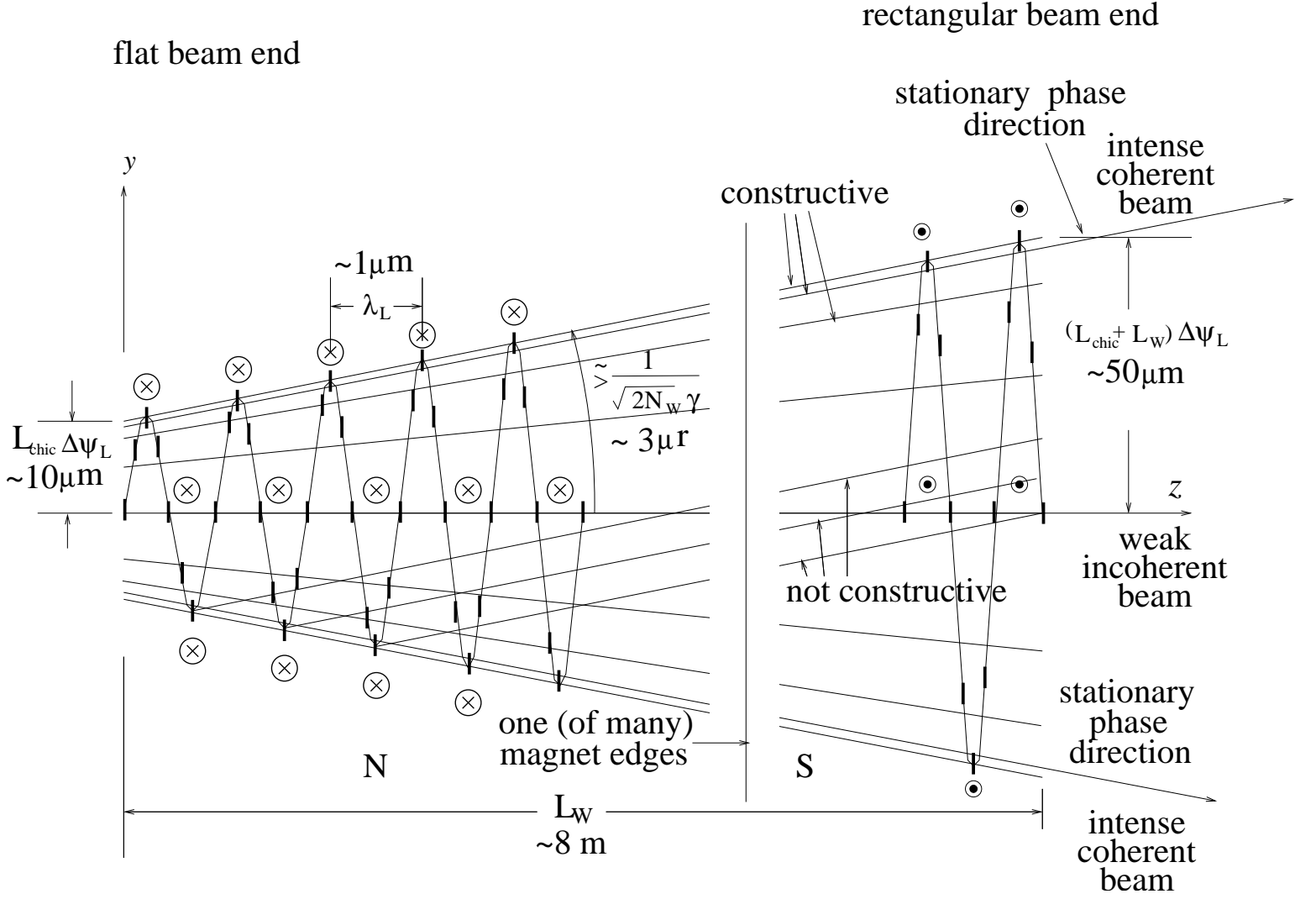


FIGURE 6. The vertically-divergent electron beam, viewed from the side, as it passes through an undulator which deflects the beam in and out of the plane of the page. Note the vast distortion of the scales. There are hundreds of north/south magnetic field reversals along the length of the undulator, and there are ten million up-down electron beam oscillation periods.

0.1. Bunch Charge and Current Achievable in CESR-X. In 1981 the maximum number of electrons per charge in CESR was $N_e = 5.5e11$, at bunch length $\sigma_z = 2.5$ cm. The limit then was set by pressure rise in the (warm) RF cavity. In 1994 the maximum single bunch charge in CESR, with superconducting RF cavities, was 44 ma in a single bunch (meaning $N_e = 7.1e11$). The limit was set by heating of components—strict proportionality to number of bunches multiplied by current-squared per bunch. In 2000, $N_e = 5.8e11$.

(8)

$$\frac{\text{wall heating power}}{m} = 1.225 \frac{1}{4\pi^2 r} \left(\frac{c}{\sigma_z} \right)^{3/2} \sqrt{\frac{\mu_0 \rho}{2}} \frac{I_{\text{av.}}^2}{M f_0}.$$

Here r is the shortest distance to the wall, ρ is the wall resistivity, and f_0 is the revolution frequency. The peak charge per bunch we can anticipate for $\sigma_z = 3$ mm is $N_e = 1.6 \times 10^{11}$. At $\sigma_z = 10$ mm the limit would be $N_e = 3.0 \times 10^{11}$.

Reference Conditions: $N_e = 10^{11}$, $\sigma_z = 3$ mm, $E_\gamma = 10$ keV.

Pulling out all the stops would result in $\widetilde{N}_e \approx 6 \times 10^{11}$. Expressed in coulombs, $Q_e \approx 100$ nC. This is 100 times greater than the bunch charge for the so-called 4th generation linac-based FEL's, like the SLAC, LCLS, and (though, of its intended applications, the comparison is only appropriate for pump-probe experiments) 1000 times greater than the charge per bunch of the Cornell ERL.

0.2. Can CESR-X Operate as an FEL?

At 3 mm bunch length, $\widetilde{N}_e = 10^{11}$, the peak current is

$$(9) \quad \hat{I} = \frac{Q_e e c}{\sqrt{2l_e l_e}} \approx 640 \text{ A}.$$

This is substantially less, for example, than the peak current of 5000 A in the TESLA FEL. But including the factor of 6 compression potentially available would roughly make up the deficit.

The product of transverse bunch dimensions in CESR-X (with CESR-C wigglers) are also comparable to FEL bunch dimensions.

G_0 , intensity gain applied to an electromagnetic wave in a single pass through an N_w -period, strength K_w , undulator;

$$(10) \quad G_0 = 65 N_w^2 \frac{\hat{I}}{I_A} \frac{\xi}{\gamma} (J_0(\xi) - J_1(\xi))^2 \approx 8.1.$$

Here $\xi = K_w^2 / (4 + 2K_w^2)$ and $I_A = 1.7 \times 10^4 \text{ A}$ is the so-called Alfvén current. Being greater than 1, this suggests there will be at least some superradiance. Another factor of 15, coming from increased charge per bunch, and bunch compression guarantees healthy laser action, especially because K_w can also be increased. i.e. E_γ decreased.

An FEL parameter ρ , defined by different authors, is regarded as a more-or-less standard parameterization. Emma defines ρ by

$$(11) \quad \rho_{\text{Emma}} = \frac{1}{4} \left(\frac{1}{2\pi} \frac{\hat{I}}{I_A} \frac{\lambda_w^2}{\beta \pi \epsilon_N} \frac{K_w^2}{\gamma^2} \right)^{1/3},$$

where β is the Twiss lattice function at the undulator and $\epsilon_N = \gamma \epsilon$ is the invariant emittance of the beam, which is assumed to be round. Emma gives a necessary condition for FEL operation to be

$$(12) \quad \sigma_\delta < \rho_{\text{Emma}}.$$

CESR-X/FEL in reference conditions fails, though only by a factor of two, to meet this condition.

Conclusion: it seems certain that the FEL threshold can be met

Conclusions

See abstract.

Anything “they” can do we could (eventually) do better with CESR-X. “They” means Brookhaven, Stanford, Argonne, ERL and most FEL’s, etc.

An FEL with higher energy, e.g. $\gamma = 3 \times 10^4$, can give harder x-rays.

A larger radius, or stronger focusing, ring could be more brilliant.

Physics advances are sure to facilitate advances in other sciences.